

## Study of Cr-SnO<sub>2</sub> ceramic pigment and of Ti/Sn ratio on formation and coloration of these materials

M.A. Tena\*, S. Meseguer, C. Gargori, A. Forés, J.A. Badenes, G. Monrós

*Inorganic Chemistry Area, Inorganic and Organic Chemistry Department, Jaume I University, Apdo, 224, E-12071 Castellón, Spain*

Received 11 December 2005; received in revised form 27 March 2006; accepted 1 April 2006

Available online 30 June 2006

### Abstract

In this study, Cr<sub>x</sub>Sn<sub>1-x</sub>O<sub>2</sub> ( $0 \leq x \leq 0.06$ ) and Cr<sub>0.03</sub>Sn<sub>0.97-y</sub>Ti<sub>y</sub>O<sub>2</sub> ( $0 < y \leq 0.97$ ) compositions were synthesized by the ceramic method and characterized by X-ray diffraction, UV–vis spectroscopy and CIE *L\*a\*b\** (Commission Internationale de l’Eclairage *L\*a\*b\**) parameters measurements. From Cr<sub>x</sub>Sn<sub>1-x</sub>O<sub>2</sub> samples fired at 1600 °C/1 h,  $x = 0.03$  was established as the composition limit of formation of solid solutions. When  $x \leq 0.01$ , better coloration of glazed tiles were obtained from short thermal treatment (1400 °C/1 h or 1600 °C/1 h) than from long thermal treatment (1400 °C/24 h). When  $0.01 < x < 0.06$  small variations of color in glazed tiles were obtained from samples fired at 1400 °C/24 h and 1600 °C/1 h. From Cr<sub>0.03</sub>Sn<sub>0.97-y</sub>Ti<sub>y</sub>O<sub>2</sub> compositions, a better purple color was obtained when  $y = 0.02$  (Ti/Sn  $\sim 2.1 \times 10^{-2}$ ) than when  $y = 0$ .

© 2006 Elsevier Ltd. All rights reserved.

**Keywords:** Powders-solid state reaction; Spectroscopy; Color; Traditional ceramics; SnO<sub>2</sub>; Pigments

### 1. Introduction

SnO<sub>2</sub> is a n-type semiconductor oxide and has been studied as gas sensor,<sup>1</sup> catalyst<sup>2</sup> and ceramic pigment.<sup>3</sup> The SnO<sub>2</sub>-based catalysts modified by Fe, Cr and Mn show generally higher activity than the unmodified SnO<sub>2</sub>. XRD analysis indicates that Fe, Cr and Mn cations could be incorporated into the lattice of rutile SnO<sub>2</sub> (cassiterite) to form solid solutions.<sup>4</sup> SnO<sub>2</sub> is used as a host lattice for ceramic pigments, e.g. Sn/Cr purple,<sup>5</sup> Sn/V yellows<sup>6</sup> and Sn/Sb blue-greys.<sup>7</sup>

Chrome Tin Cassiterite is an inorganic pigment (11-22-5 DCMA, Dry Color Manufacturers Association<sup>8</sup>) with chemical formula (Sn,Cr)O<sub>2</sub>. It is a reaction product of high temperature calcination in which tin(IV) oxide and chromium(III) oxide in varying amounts are homogeneously and ionically interdiffused to form a crystalline matrix of cassiterite. The violet color of Cr-SnO<sub>2</sub> can only be developed in the narrow range of the Cr<sub>2</sub>O<sub>3</sub> content. Ren et al.<sup>9</sup> studied chromium-based ceramic colors. Cr<sup>4+</sup> in SnO<sub>2</sub> produced a purple color. They established that the concentration of chromium dissolved in SnO<sub>2</sub> is less than 2.8 mol% as CrO<sub>2</sub>, that is 1.6 wt% as Cr<sub>2</sub>O<sub>3</sub>. The solubility limit

of chromium in the inner part of the SnO<sub>2</sub> grain is considerably smaller than 1.6 wt% as Cr<sub>2</sub>O<sub>3</sub>. From lattice constants, 1.4 mol% CrO<sub>2</sub> (0.8 wt% as Cr<sub>2</sub>O<sub>3</sub>) was reported as the solubility limit value. From reflectance spectra, these authors showed the overlapping of Cr<sup>3+</sup> spectrum with Cr<sup>4+</sup> spectrum in the 0.83 wt% sample. From susceptibility measurements, they established the Cr<sup>3+</sup> ratio of 18% to total chromium in the 0.193 wt% sample. Not only the solubility limit of chromium, but also the Cr<sup>3+</sup>/Cr<sup>4+</sup> ratio is an important piece of information in designing ceramic colors. Oxidation state and localization of chromium ions in Cr-doped cassiterite were studied by Ocaña and co-workers<sup>5</sup> Cr/SnO<sub>2</sub> molar ratio = 0.046 produced the optimum pigments.<sup>10</sup> These authors concluded that most chromium species in this pigment were not dissolved in the cassiterite lattice. The presence of a pre-edge peak in the XANES spectrum at Cr K-edge confirmed that a certain amount of the total chromium ions was in the tetravalent state with an atomic environment similar to that in CrO<sub>2</sub>. Cr(III) antiferromagnetic clusters and a small amount of ferromagnetic CrO<sub>2</sub> nanoparticles were detected from magnetic data.

Chromium dissolves as Cr<sup>3+</sup> and Cr<sup>4+</sup> in rutile type oxides. Cordischi et al.<sup>11</sup> studied the properties of VI B transition metal ions in rutile TiO<sub>2</sub> solid solutions. When mixtures of MO<sub>2</sub> (M=Cr, Mo, or W) and TiO<sub>2</sub> were heated in vacuo at 1173–1273 K, solid solutions formed. Chromium entered into

\* Corresponding author. Tel.: +34 964728249; fax: +34 964728214.  
E-mail address: [tena@qio.uji.es](mailto:tena@qio.uji.es) (M.A. Tena).

the rutile structure up to  $\approx 4\%$  (Cr atoms/100 Ti atoms), as  $\text{Cr}^{3+}$  ( $3d^3$  ion). At higher chromium content compounds of general formula  $\text{Ti}_{n-2}\text{Cr}_2\text{O}_{2n-1}$  were found. The treatment in air at 1273 K slightly decreases the solubility limit (3%) and changed the color (from orange to dark brown) because a non-stoichiometric compound,  $\text{CrO}_x$ , formed on the titania surface. The formation of the compound  $\text{CrO}_x$  was confirmed by Ishida et al.<sup>12</sup> These authors studied chemical state and coloration of chromium in rutile. Cr-doped  $\text{TiO}_2$  had a yellow color resulting from dissolved  $\text{Cr}^{3+}$  when the Cr content was less than 0.1 wt%  $\text{CrO}_3$ . Maple color produced by both  $\text{Cr}^{3+}$  and  $\text{Cr}^{4+}$  dissolved in  $\text{TiO}_2$  was obtained with a Cr content equal to 0.2 wt%  $\text{CrO}_3$ . Black color caused by undissolved  $\text{CrO}_{3-x}$  ( $x=0.4-0.8$ ) on the  $\text{TiO}_2$  grains was obtained when the Cr content was 1 wt%  $\text{CrO}_3$ . Croft and Fuller<sup>13</sup> attempted to obtain new pigments by doping ions into solid solutions of  $\text{SnO}_2$  and  $\text{TiO}_2$ . Their attempt was unsuccessful in the case of  $\text{Cr}_2\text{O}_3\text{-Sn}_{1-x}\text{Ti}_x\text{O}_2$  system. In that study, the Cr/(Sn + Ti) ratio was 10 mol%.

From literature it is seem clear that both  $\text{Cr}^{3+}$  and  $\text{Cr}^{4+}$  are necessary to obtain violet colorations characteristics of Cr-SnO<sub>2</sub> pigment. Although the solubility of chromium in  $\text{SnO}_2$  is small, adequate colorations are obtained with chromium amount higher than the solubility limit value. There is little information about the influence of thermal treatment and their efficiency as violet-purple ceramic pigment on glazed tiles.

The aim of this study is to establish the compositional range of  $\text{Cr}_x\text{Sn}_{1-x}\text{O}_2$  samples for which the materials are purple, the influence of thermal treatment in the coloration of these materials and to determine the influence of Ti/Sn ratio on formation and coloration of these materials.

## 2. Experimental procedure

$\text{Cr}_x\text{Sn}_{1-x}\text{O}_2$  ( $0 \leq x \leq 0.06$ ) compositions were prepared by the ceramic method. The starting materials were  $\text{SnO}_2$  (Panreac) and  $\text{Cr}_2\text{O}_3$  (Merck). The appropriate amounts of the starting materials were mixed and homogenized in acetone in a planetary ball mill for 20 min. Residual acetone was removed by evaporation. All dried samples were put into refractory crucibles and fired. In order to establish the temperature range in thermal treatment of samples, a composition ( $\text{Cr}_{0.005}\text{Sn}_{0.995}\text{O}_2$ ) with chromium amount smaller than the solubility limit value of  $\text{Cr}^{4+}$  in  $\text{SnO}_2$  reported by Ren et al. (1.4 mol%  $\text{CrO}_2$ ) was chosen. This composition ( $\text{Cr}_{0.005}\text{Sn}_{0.995}\text{O}_2$ ) was fired at 600, 700, 800, 900, 1000, 1100, 1200, 1300, 1400 and 1600 °C for 1 h of soaking times at each temperature. Violet coloration characteristic of Cr-SnO<sub>2</sub> pigment was obtained when  $T \geq 1400$  °C. Thus,  $\text{Cr}_x\text{Sn}_{1-x}\text{O}_2$  ( $0 \leq x \leq 0.06$ ) samples were fired at 1400 °C/1 h, 1400 °C/24 h and 1600 °C/1 h.

From the characterization of these samples, when  $\text{TiO}_2$  were added to  $\text{Cr}_x\text{Sn}_{1-x}\text{O}_2$  compositions  $x=0.03$  was chosen to compare results. The chromium amount in this composition exceeds the concentration of chromium dissolved in  $\text{SnO}_2$  (2.8 mol% as  $\text{CrO}_2$ ) proposed by Ren et al.<sup>9</sup> but Cr/Sn molar ratio is smaller than Cr/Sn molar ratio = 0.046 proposed by Ocaña and co-workers<sup>5</sup> Thus,  $\text{Cr}_{0.03}\text{Sn}_{0.97-y}\text{Ti}_y\text{O}_2$  ( $0 \leq y \leq 0.97$ ) compositions were prepared by the ceramic method and fired at

1000 °C/24 h and 1400 °C/24 h. The starting materials were  $\text{TiO}_2$  anatase (Panreac),  $\text{SnO}_2$  (Panreac) and  $\text{Cr}_2\text{O}_3$  (Merck).

Thermogravimetric analysis (TG) were carried out in a Mettler Toledo instrument in a synthetic air atmosphere using alumina crucible and a heating rate 5 °C/min.

The resulting materials were examined with a Siemens D5000D X-ray diffractometer with Cu K $\alpha$  radiation to study the development of the crystalline phases at different temperatures. In fired samples at 1400 and 1600 °C, a structure profile refinement was carried out by the RIETVELD method<sup>14</sup> with the data obtained in the [20–100]  $2\theta^\circ$  Bragg angle interval. The experimental conditions used were Cu K $\alpha$  radiation, graphite monochromator, 40 kV, 30 mA, 2° divergence slit, 0.06 detector slit, step size of 0.02  $2\theta^\circ$  and 14 s for each step.

UV–vis–NIR spectroscopy (diffuse reflectance) allows the presence of  $\text{Cr}^{3+}$  and  $\text{Cr}^{4+}$  in the prepared specimens to be studied. A Lambda 2000 Perkin-Elmer spectrophotometer was used to obtain the UV–vis–NIR (ultraviolet visible near infrared) spectra in the 200–1400 nm range.

In order to test their efficiency as violet-purple ceramic pigment, the compositions fired at 1400 °C/1 h, 1400 °C/24 h and 1600 °C/1 h were 5% weight enamelled with  $\text{K}_2\text{O-ZnO-SiO}_2$  glazes, usual in ceramic tile industry. Glazed tiles were fired for 5 min at 1085 °C for the single-firing glaze in a cycle of 60 min (cold-to-cold).

CIE  $L^*a^*b^*$  color parameter measurements,<sup>15</sup> conducted with a Perkin-Elmer colorimeter using a standard illuminant D, were used to differentiate the samples in terms of color.  $L^*$  is the lightness axis (black (0)  $\rightarrow$  white (100)),  $a^*$  is the green (–)  $\rightarrow$  red (+) axis and  $b^*$  is the blue (–)  $\rightarrow$  yellow (+) axis. The measurements were made on powdered samples and on glazed tiles.

## 3. Results and discussion

Cassiterite is the only crystalline phase obtained in  $\text{Cr}_{0.005}\text{Sn}_{0.995}\text{O}_2$  fired sample. Observed color of  $\text{Cr}_{0.005}\text{Sn}_{0.995}\text{O}_2$  fired composition and CIE  $L^*a^*b^*$  color parameters are shown in Table 1. Representative UV–vis spectra are shown in Fig. 1. The coloration of samples, according with spectra indicates that Cr(III) is present in raw sample ( $\text{Cr}_2\text{O}_3$ , green), Cr(VI) is present in sample fired at 600 and

Table 1  
Observed color and CIE  $L^*a^*b^*$  color parameters in  $\text{Cr}_{0.005}\text{Sn}_{0.995}\text{O}_2$  fired composition (powdered samples)

$T$ (°C)	Observed color	$L^*$	$a^*$	$b^*$
600	Yellow	87.04	–2.51	5.47
700	Yellow	85.58	–2.07	4.96
800	Pink	84.25	0.37	2.2
900	Pink	79.07	3.2	–2.34
1000	Pink	77.5	4.47	–3.84
1100	Pink	78.04	3.76	–2.88
1200	Pink	79.08	2.85	–0.1
1300	Pink	74.34	6.07	–3.08
1400	Violet	66.71	10.75	–8.82
1600	Violet	51.88	12.75	–10.81

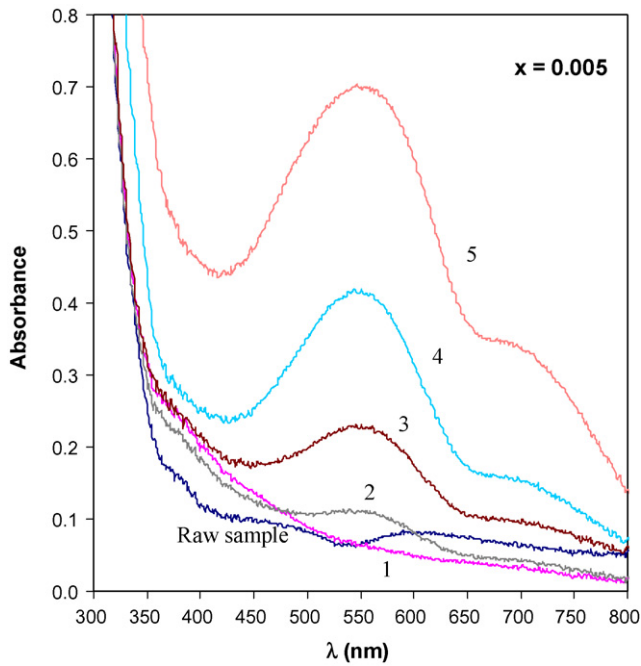


Fig. 1. UV-vis spectra of  $\text{Cr}_{0.005}\text{Sn}_{0.995}\text{O}_2$  raw sample and sample fired at 600 °C (1), 800 °C (2), 1100 °C (3), 1400 °C (4) and 1600 °C (5).

700 °C (yellow) and Cr(IV) is present in fired samples when  $T \geq 800$  °C (pink and violet). In the raw sample, bands around 600 and 470 nm are assigned to  $\text{Cr}^{3+}$  in an octahedral site ( $\text{Cr}_2\text{O}_3$ ):  $^4\text{A}_2(\text{F}) \rightarrow ^4\text{T}_2(\text{F})$ , first octahedral  $\text{Cr}^{3+}$  transition and  $^4\text{A}_2(\text{F}) \rightarrow ^4\text{T}_1(\text{F})$ , second octahedral  $\text{Cr}^{3+}$  transition. In fired sample at 600 and 700 °C, absorption at 390 nm is assigned to the presence of chromates. When  $T \geq 800$  °C, the location of maximum absorption is in 550 nm. This absorption band at 550 nm is assigned to  $\text{Cr}^{4+}$  in an octahedral site, according with literature.<sup>9</sup> The absorption in 550 nm increases when temperature increases.

From these results,  $T \geq 1400$  °C was established as firing temperature range to obtain violet ceramic pigments in this system ( $L^* < 70$ ,  $a^* > 8$ ,  $b^* < -8$ ).

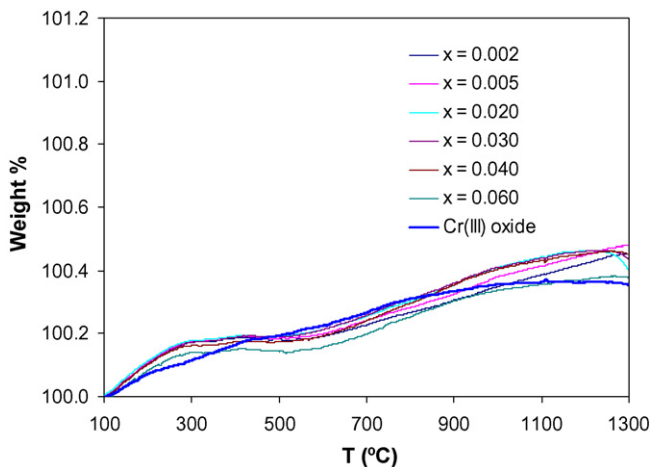


Fig. 2. TG curves of  $\text{Cr}_2\text{O}_3$  and  $\text{Cr}_x\text{Sn}_{1-x}\text{O}_2$  samples with  $0.002 \leq x \leq 0.06$ .

Table 2

Crystalline phases in  $\text{Cr}_x\text{Sn}_{1-x}\text{O}_2$  samples fired at 1400 and 1600 °C

$x$	1400 °C/1 h	1400 °C/24 h	1600 °C/1 h
0.002	C (s)	C (s)	C (s)
0.005	C (s)	C (s)	C (s)
0.01	C (s), E (vw)	C (s)	C (s)
0.02	C (s), E (vw)	C (s)	C (s)
0.03	C (s), E (vw)	C (s), E (vw)	C (s)
0.04	C (s), E (vw)	C (s), E (vw)	C (s), E (vw)
0.05	C (s), E (vw)	C (s), E (vw)	C (s), E (vw)
0.06	C (s), E (vw)	C (s), E (vw)	C (s), E (vw)

Crystalline phases: C=cassiterite, E= $\text{Cr}_2\text{O}_3$ . Diffraction peak intensity: s=strong, m=medium, w=weak, vw=very weak.

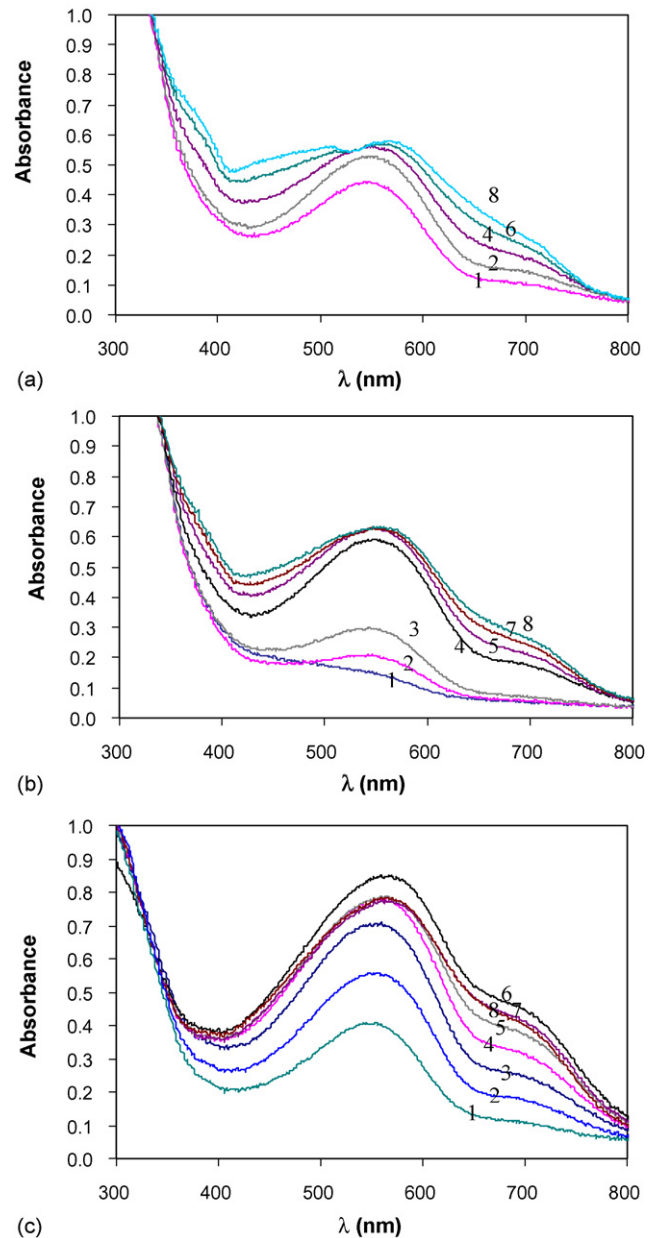


Fig. 3. UV-vis spectra of glazed tiles from  $\text{Cr}_x\text{Sn}_{1-x}\text{O}_2$  samples with (1)  $x=0.002$ , (2)  $x=0.005$ , (3)  $x=0.010$ , (4)  $x=0.020$ , (5)  $x=0.030$ , (6)  $x=0.040$ , (7)  $x=0.050$  and (8)  $x=0.060$  fired at (a) 1400 °C/1 h, (b) 1400 °C/24 h and (c) 1600 °C/1 h.

For the production of these pigments,  $\text{Cr}_2\text{O}_3$  can be used as precursor. The use of chromates as precursors is not necessary. Chromates are obtained about 600–700 °C from  $\text{Cr}_2\text{O}_3$ . This is in accordance with results in a previous study.<sup>16</sup> In this study was concluded that chromate amount was not dependent of the chromium precursor but depends of the allowed reactivity level and the reaction media.

Fig. 2 shows the TG curves of  $\text{Cr}_x\text{Sn}_{1-x}\text{O}_2$  samples. A weight increase from 100 to 1250 °C is detected in all TG curve. It could be associated with the oxidation of Cr(III). When  $200 < T < 350$  and  $900 < T < 1300$  °C, the increase is higher in  $\text{Cr}_x\text{Sn}_{1-x}\text{O}_2$  samples than in  $\text{Cr}_2\text{O}_3$ . Chromium oxidation is helped in presence of  $\text{SnO}_2$ . A weight loss in samples with  $x \geq 0.01$  is detected when  $T > 1250$ . It can be associated with volatilization of chromium or reduction of chromium in samples.

Table 2 shows crystalline phase evolution with temperature in  $\text{Cr}_x\text{Sn}_{1-x}\text{O}_2$  ( $0 \leq x \leq 0.06$ ) samples. Cassiterite is the only crystalline phase obtained in these samples fired at 1400 °C/24 h or 1600 °C/1 h when  $x < 0.03$  or  $x < 0.04$ , respectively. Together with cassiterite phase  $\text{Cr}_2\text{O}_3$  is detected when  $x \geq 0.01$  in these samples fired at 1400 °C/1 h, when  $x \geq 0.03$  in samples fired at 1400 °C/24 h and when  $x \geq 0.04$  in samples fired at 1600 °C/1 h. This residual phase masks the violet color in glazed tiles. From samples fired at 1400 °C/1 h and  $x > 0.02$ , gray color is obtained in glazed tiles. Fig. 3 shows representative UV–vis spectra of glazed tiles from samples fired at 1400 °C/1 h, 1400 °C/24 h and 1600 °C/1 h. The increase of absorbance around 600 and 470 nm when  $x > 0.05$  (Fig. 3a) is in accordance with the presence of  $\text{Cr}_2\text{O}_3$  ( $\text{Cr}^{3+}$  in an octahedral site) detected by XRD (Table 2). The absorbance in 550 nm indicates the presence of  $\text{Cr}^{4+}$  in all samples. Higher absorbance at 550 nm from samples fired at 1600 °C/1 h is detected than from samples fired at 1400 °C/24 h

(or 1400 °C/1 h) (Fig. 3c). From results, 1600 °C/1 h might be established as firing temperature to obtain violet-purple ceramic pigments in this system when  $x < 0.02$ . When  $x \geq 0.02$ , it is observed that blue component in color of glazed tiles ( $b^*(-)$ ) changes with fired temperature of samples (Table 3) while red component ( $a^*(+)$ ) is similar from samples fired at 1400 °C/24 h and in samples fired at 1600 °C/1 h. This change of coloration can be attributed to oxidation of  $\text{Cr}_2\text{O}_3$  into glazed tiles.

No appreciable changes are detected in cassiterite unit cell parameters in  $\text{Cr}_x\text{Sn}_{1-x}\text{O}_2$  samples fired at 1400 °C/24 h. A light decrease of unit cell parameters is detected from these samples fired at 1600 °C/1 h (Fig. 4). It is in agreement with the replacement of tin by the  $\text{Cr}^{4+}$  ion ( $r(\text{Sn}^{4+}) = 0.69$  Å and  $r(\text{Cr}^{4+}) = 0.55$  Å from Shannon radii for octahedral coordination). This fact indicates that solid solutions with cassiterite structure are formed. The decrease of the  $a$  parameter is smaller than the decrease of the  $c$  parameter. Therefore, a distortion in the cassiterite structure is obtained with these solid solutions. The decrease of unit cell parameters is detected when  $0 < x \leq 0.03$ . This result and the presence of  $\text{Cr}_2\text{O}_3$  as residual crystalline phase detected by XRD (Table 2) allow to establish the limit of solid solutions about  $x = 0.03$  from samples fired at 1600 °C/1 h.

Table 4 shows crystalline phases detected in  $\text{Cr}_{0.03}\text{Sn}_{0.97-y}\text{Ti}_y\text{O}_2$  ( $0 < y \leq 0.97$ ) samples and their evolution with temperature. From these samples, cassiterite only phase is obtained when  $y < 0.485$  at 1400 °C/24 h. Rutile only phase is obtained when  $y > 0.77$  at 1400 °C/24 h. Two crystalline phases with tetragonal structure are detected when  $0.485 \leq y \leq 0.770$  in samples fired at 1400 °C/24 h. Although rutile is isostructural with cassiterite, because of the great difference between  $\text{Ti}^{4+}$  and  $\text{Sn}^{4+}$  ionic radius, it is possible to distinguish between the cassiterite phase, rutile phase and the two-phase mixture. Fig. 5 shows XRD patterns of samples with

Table 3  
CIE  $L^*a^*b^*$  color parameters in  $\text{Cr}_x\text{Sn}_{1-x}\text{O}_2$  samples

$x$	Samples fired at 1400 °C/1 h			Samples fired at 1400 °C/24 h			Samples fired at 1600 °C/1 h		
	$L^*$	$a^*$	$b^*$	$L^*$	$a^*$	$b^*$	$L^*$	$a^*$	$b^*$
0.002	68.60	9.99	−8.32	75.28	7.43	−5.13	62.94	12.18	−10.21
0.005	66.71	10.75	−8.82	67.72	11.70	−9.37	51.88	12.75	−10.81
0.010	66.59	11.10	−8.88	58.94	14.33	−12.03	50.62	11.25	−9.52
0.020	65.87	9.85	−7.98	51.99	11.51	−9.66	50.06	9.49	−7.55
0.030	66.03	8.64	−7.09	49.22	10.39	−8.69	46.54	9.01	−6.96
0.040	65.66	7.93	−6.46	51.65	10.13	−8.44	49.45	7.87	−6.42
0.050	65.54	7.25	−5.76	48.37	9.05	−7.71	46.64	7.07	−5.60
0.060	65.33	6.74	−5.42	49.04	8.55	−7.20	44.02	6.56	−5.01
Glazed tiles from samples fired at 1400 °C/1 h									
	$L^*$	$a^*$	$b^*$	$L^*$	$a^*$	$b^*$	$L^*$	$a^*$	$b^*$
0.002	69.87	17.29	−7.69	84.41	4.90	8.73	72.74	15.61	−8.12
0.005	64.63	18.47	−11.43	82.19	7.80	1.87	61.28	19.83	−16.43
0.010	64.96	17.88	−9.15	76.97	11.95	−0.60	55.80	20.73	−18.43
0.020	61.53	14.80	−8.09	61.14	18.72	−11.59	52.57	18.93	−19.99
0.030	59.72	12.21	−6.52	58.52	17.02	−9.14	49.93	16.88	−19.86
0.040	59.55	10.32	−3.87	58.93	16.74	−7.73	46.49	16.05	−21.86
0.050	57.39	7.63	−3.71	58.08	14.29	−7.21	50.47	13.46	−20.34
0.060	58.27	7.13	−1.70	56.65	12.45	−6.07	50.33	13.80	−18.85



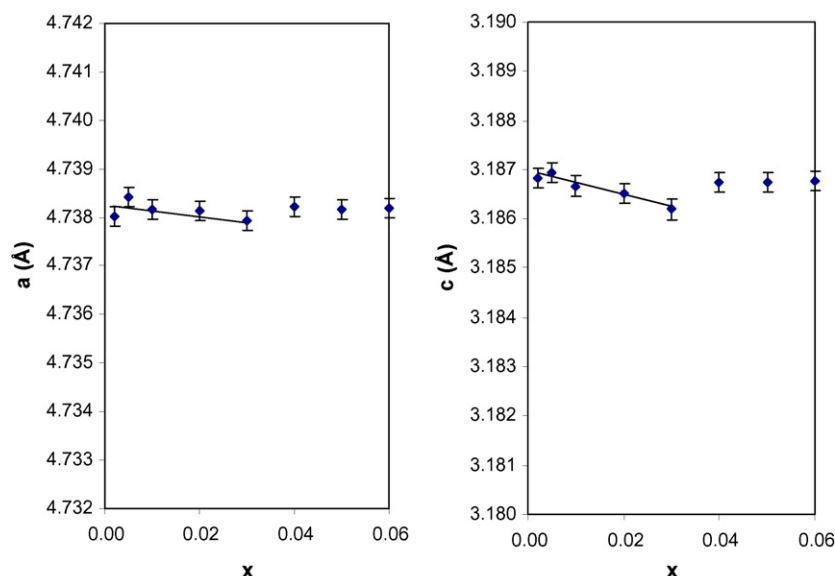


Fig. 4. Unit cell parameters of cassiterite phase for  $\text{Cr}_x\text{Sn}_{1-x}\text{O}_2$  ( $0 < x \leq 0.06$ ) samples fired at  $1600^\circ\text{C}/1\text{ h}$ .

Table 4  
Crystalline phase evolution in  $\text{Cr}_{0.03}\text{Ti}_y\text{Sn}_{0.97-y}\text{O}_2$  samples with temperature

y	Nominal composition	1000 °C/24 h	1400 °C/24 h
0.000	$\text{Cr}_{0.03}\text{Sn}_{0.970}\text{O}_2$	C (s), E (vw)	C (s), E (vw)
0.020	$\text{Cr}_{0.03}\text{Ti}_{0.02}\text{Sn}_{0.95}\text{O}_2$	C (s)	C (s)
0.070	$\text{Cr}_{0.03}\text{Ti}_{0.070}\text{Sn}_{0.90}\text{O}_2$	C (s)	C (s)
0.270	$\text{Cr}_{0.03}\text{Ti}_{0.270}\text{Sn}_{0.70}\text{O}_2$	C (s), R (w)	C (s)
0.485	$\text{Cr}_{0.03}\text{Ti}_{0.485}\text{Sn}_{0.485}\text{O}_2$	C (m), R (w)	C (m), R (w)
0.770	$\text{Cr}_{0.03}\text{Ti}_{0.770}\text{Sn}_{0.20}\text{O}_2$	R (s), C (w)	R (s), C (vw)
0.850	$\text{Cr}_{0.03}\text{Ti}_{0.850}\text{Sn}_{0.12}\text{O}_2$	R (s)	R (s)
0.970	$\text{Cr}_{0.03}\text{Ti}_{0.970}\text{O}_2$	R (s)	R (s)

Crystalline phases: C=cassiterite:  $(\text{Cr},\text{Sn},\text{Ti})\text{O}_2$  solid solution with  $\text{SnO}_2$ -rich composition. R=rutile:  $(\text{Cr},\text{Sn},\text{Ti})\text{O}_2$  solid solution with  $\text{TiO}_2$ -rich composition, E:  $\text{Cr}_2\text{O}_3$ . Diffraction peak intensity: s=strong, m=medium, w=weak, vw=very weak.

$y=0.270$ ,  $y=0.485$  and  $y=0.770$  fired at  $1400^\circ\text{C}/24\text{ h}$ . The variation of unit cell parameters with composition confirms the formation of two  $(\text{Cr},\text{Ti},\text{Sn})\text{O}_2$  solid solutions (Table 5). One of them is  $(\text{Cr},\text{Sn},\text{Ti})\text{O}_2$  solid solution with  $\text{SnO}_2$ -rich compositions and the another one is  $(\text{Cr},\text{Sn},\text{Ti})\text{O}_2$  solid solution with

$\text{TiO}_2$ -rich compositions. These unit cell parameters decrease with composition according to the replacement of a great ion ( $\text{Sn}^{4+}$ ) by a smaller one ( $\text{Ti}^{4+}$ ) when solid solutions are formed. The contraction of “c” and “a” parameters is observed to be different. When y increases, the value of  $c/a$  ratio decreases in cassiterite solid solutions ( $y < 0.3$ ) and it increases in rutile solid solutions ( $y > 0.5$ ). Phase development and the variation of unit cell parameters with temperature indicate that an immiscibility dome is present in  $(\text{Cr},\text{Ti},\text{Sn})\text{O}_2$  solid solutions at  $1400^\circ\text{C}$ . From these results it is possible to establish the solubility limits in  $y \approx 0.3$  and  $y \approx 0.8$  for prepared cassiterite and rutile solid solutions, respectively, at  $1400^\circ\text{C}$ . The great difference between  $\text{Ti}^{4+}$  and  $\text{Sn}^{4+}$  ionic radius masks the small variation of unit cell parameters due to the presence of chromium in these solid solutions.

Fig. 6 shows visible spectra of  $\text{Cr}_{0.03}\text{Sn}_{0.97-y}\text{Ti}_y\text{O}_2$  ( $0 < y \leq 0.97$ ) samples fired at  $1400^\circ\text{C}/24\text{ h}$  and visible spectra of glazed tiles from these samples when  $y < 0.3$ . In these spec-

Table 5  
Unit cell parameters of  $\text{Cr}_{0.03}\text{Ti}_y\text{Sn}_{0.97-y}\text{O}_2$  samples fired at  $1400^\circ\text{C}/24\text{ h}$

y	a (Å)	c (Å)	c/a
0.00	4.7372(1) <sup>a</sup>	3.1864(1) <sup>a</sup>	0.6726 <sup>a</sup>
0.02	4.73401(1) <sup>a</sup>	3.1823(1) <sup>a</sup>	0.6722 <sup>a</sup>
0.07	4.72848(1) <sup>a</sup>	3.1735(1) <sup>a</sup>	0.6711 <sup>a</sup>
0.27	4.7022(2) <sup>a</sup>	3.1531(2) <sup>a</sup>	0.6705 <sup>a</sup>
0.485	4.7016(3) <sup>a</sup>	3.1574(2) <sup>a</sup>	0.6715 <sup>a</sup>
	4.6542(4) <sup>b</sup>	2.9651(4) <sup>b</sup>	0.6371 <sup>b</sup>
0.77	4.6273(2) <sup>b</sup>	2.9639(3) <sup>b</sup>	0.6405 <sup>b</sup>
0.85	4.6158(1) <sup>b</sup>	2.9603(1) <sup>b</sup>	0.6413 <sup>b</sup>
0.97	4.5970(1) <sup>b</sup>	2.9584(1) <sup>b</sup>	0.6435 <sup>b</sup>

<sup>a</sup> Cassiterite solid solution.

<sup>b</sup> Rutile solid solution.

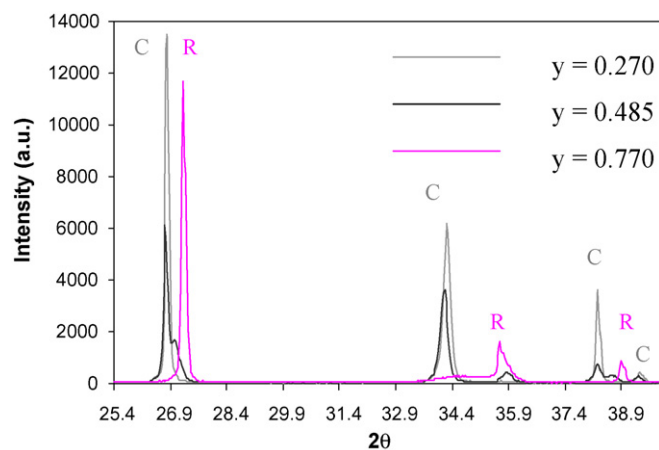


Fig. 5. XRD patterns  $\text{Cr}_{0.03}\text{Sn}_{0.97-y}\text{Ti}_y\text{O}_2$  of samples with  $y=0.270$ ,  $y=0.485$  and  $y=0.770$  fired at  $1400^\circ\text{C}/24\text{ h}$ .

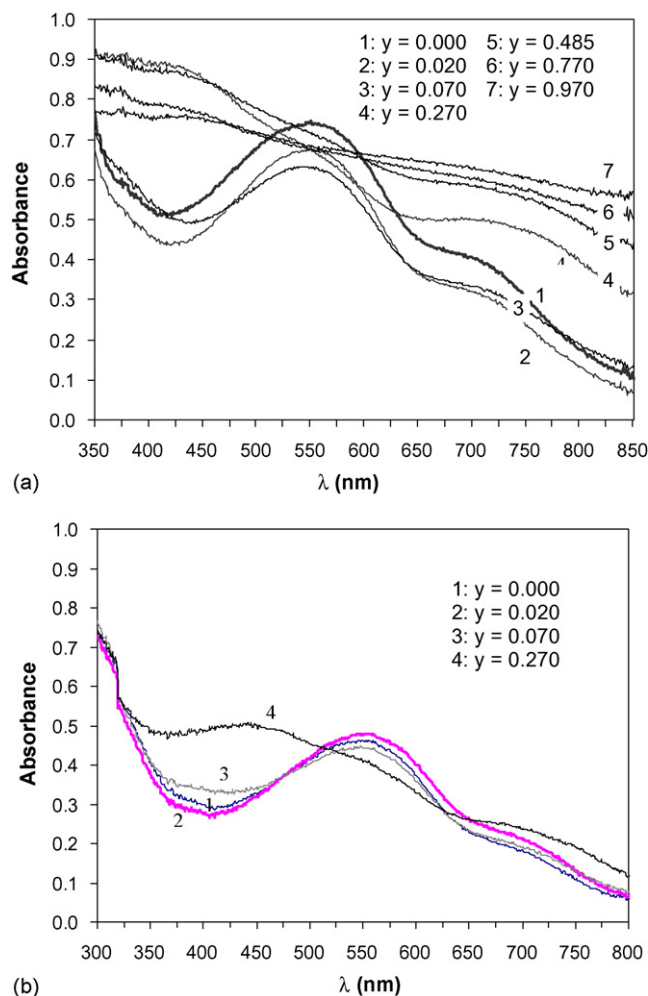


Fig. 6. UV-vis spectra of  $\text{Cr}_{0.03}\text{Sn}_{0.97-y}\text{Ti}_y\text{O}_2$  ( $0 < y \leq 0.97$ ) samples fired at  $1400^\circ\text{C}/24\text{ h}$  (a) powdered samples and (b) glazed tiles.

tra, the band in 550 nm assigned to  $\text{Cr}^{4+}$  in an octahedral site is detected in samples with  $y < 0.10$  ( $\text{SnO}_2$ -rich compositions). When titanium amount increases, a very broad absorption in 350–850 nm range is present in spectra. This broad absorption is due to the presence of Cr ions in different valence states.<sup>9</sup> The incorporation of titanium modifies the crystal field strength and  $\text{Cr}^{4+}$  is not the dominant dissolved specie in prepared solid solutions with  $y > 0.10$ .

Table 6 shows the variation of CIE  $L^*$ ,  $a^*$  and  $b^*$  parameters of raw samples and samples fired at 1000 and  $1400^\circ\text{C}$ . In fired samples at  $1400^\circ\text{C}$ , green coloration of initial mixtures changes to purple coloration when  $y < 0.10$  and to brown coloration when  $y > 0.10$ . In fired samples at  $1000^\circ\text{C}$ , the coloration is very light. Thus, coloration of prepared materials is purple when the predominant specie is  $\text{Cr}^{4+}$  ( $y < 0.10$ ). The best purple color (minimum  $b^*$  and maximum  $a^*$ ) is obtained in sample with  $y = 0.02$ . A small increase of Ti/Sn ratio improves the purple color but when  $y > 0.07$  the coloration of materials has a tendency to brown color. From glazed tiles, the best purple color is also obtained when  $y = 0.02$ ,  $\text{Ti/Sn} = 2.1 \cdot 10^{-2}$  (Table 7). Ti/Sn ratio seems to influence on the coloration of materials because the incorporation of titanium in cassiterite solid solutions modifies

Table 6  
CIE  $L^*a^*b^*$  parameters of  $\text{Cr}_{0.03}\text{Ti}_y\text{Sn}_{0.97-y}\text{O}_2$  samples

y	Raw sample	$1000^\circ\text{C}/24\text{ h}$	$1400^\circ\text{C}/24\text{ h}$
0.000	$L^* = 84.79$ $a^* = -5.88$ $b^* = 4.27$	$L^* = 82.42$ $a^* = 2.42$ $b^* = 2.63$	$L^* = 49.22$ $a^* = 10.39$ $b^* = -8.69$
0.020	$L^* = 85.06$ $a^* = -4.87$ $b^* = 3.84$	$L^* = 84.37$ $a^* = -0.50$ $b^* = 6.48$	$L^* = 53.52$ $a^* = 15.09$ $b^* = -11.53$
0.070	$L^* = 88.42$ $a^* = -3.99$ $b^* = 3.52$	$L^* = 84.99$ $a^* = -0.90$ $b^* = 8.45$	$L^* = 55.14$ $a^* = 11.80$ $b^* = -5.78$
0.270	$L^* = 86.34$ $a^* = -5.27$ $b^* = 4.84$	$L^* = 73.65$ $a^* = 1.08$ $b^* = 11.17$	$L^* = 54.10$ $a^* = 6.86$ $b^* = 16.25$
0.485	$L^* = 88.45$ $a^* = -4.69$ $b^* = 3.83$	$L^* = 68.19$ $a^* = 1.57$ $b^* = 6.88$	$L^* = 50.62$ $a^* = 4.16$ $b^* = 11.16$
0.770	$L^* = 91.42$ $a^* = -3.81$ $b^* = 2.08$	$L^* = 59.02$ $a^* = 3.88$ $b^* = 13.96$	$L^* = 52.27$ $a^* = 1.10$ $b^* = 7.24$
0.970	$L^* = 88.30$ $a^* = -3.96$ $b^* = 1.95$	$L^* = 61.39$ $a^* = 4.51$ $b^* = 21.40$	$L^* = 51.87$ $a^* = 0.99$ $b^* = 5.61$

Table 7  
CIE  $L^*a^*b^*$  parameters in glazed tiles from  $\text{Cr}_{0.03}\text{Ti}_y\text{Sn}_{0.97-y}\text{O}_2$

Sample	Color of glazed tiles with sample addition	$L^*$	$a^*$	$b^*$
$\text{Cr}_{0.03}\text{Sn}_{0.970}\text{O}_2$	Purple	58.52	17.02	-9.14
$\text{Cr}_{0.03}\text{Ti}_{0.02}\text{Sn}_{0.95}\text{O}_2$	Purple	55.88	16.48	-15.45
$\text{Cr}_{0.03}\text{Ti}_{0.070}\text{Sn}_{0.90}\text{O}_2$	Violet	58.84	14.32	-7.88
$\text{Cr}_{0.03}\text{Ti}_{0.270}\text{Sn}_{0.70}\text{O}_2$	Brown	59.08	9.66	14.74

the crystal field of  $\text{SnO}_2$  matrix. The results indicate than compositions about of  $\text{Cr}_{0.03}\text{Sn}_{0.95}\text{Ti}_{0.02}\text{O}_2$  ( $\text{Ti/Sn} = 2.1 \times 10^{-2}$ ) may be the optimum composition to obtain purple ceramic pigments from  $\text{Cr}_{0.03}\text{Sn}_{0.97-y}\text{Ti}_y\text{O}_2$  samples.

#### 4. Conclusions

$\text{Cr}_x\text{Sn}_{1-x}\text{O}_2$  ( $0 \leq x \leq 0.03$ ) cassiterite solid solutions have been synthesized at  $1600^\circ\text{C}/1\text{ h}$ . These materials develop suitable violet-purple colorations that are stable in glazed tiles. Both temperature and soaking times influence on the development of coloration in noticeable form.  $T \geq 1400^\circ\text{C}$  has been established as firing temperature range to obtain violet ceramic pigments in this system.

Two  $(\text{Cr,Ti,Sn})\text{O}_2$  solid solutions have been characterized from  $\text{Cr}_{0.03}\text{Sn}_{0.97-y}\text{Ti}_y\text{O}_2$  samples fired at  $1400^\circ\text{C}/24\text{ h}$ . They are cassiterite solid solution with  $\text{SnO}_2$ -rich compositions and rutile solid solution with  $\text{TiO}_2$ -rich compositions. It is possible to establish the solubility limits in  $y \approx 0.3$  and  $y \approx 0.8$  for prepared cassiterite and rutile solid solutions, respectively, at  $1400^\circ\text{C}/24\text{ h}$ . Purple coloration is only obtained from cassiterite solid solutions. Ti/Sn ratio seems to influence on the coloration

of materials prepared from  $\text{Cr}_{0.03}\text{Sn}_{0.97-y}\text{Ti}_y\text{O}_2$  compositions. When Ti/Sn is small ( $\text{Ti/Sn} = 2.1 \times 10^{-2}$ ), purple coloration is better than when  $y=0.0$  ( $\text{Ti/Sn}=0$ ) in powdered samples and glazed tiles.

### Acknowledgement

We gratefully acknowledge the financial support given by M E C, MAT 2005-00507 project.

### References

1. Gao, Y., Zhao, H. B. and Zhao, B. Y., Monolayer dispersion of oxide additives on  $\text{SnO}_2$  and their promoting effects on thermal stability of  $\text{SnO}_2$  ultrafine particles. *J Mater Sci*, 2000, **35**(4), 917–923.
2. Harrison, P. G., Bailey, C. and Azelee, W., Modified tin(IV) oxide ( $\text{M/SnO}_2$   $\text{M}=\text{Cr, La, Pr, Nd, Sm, Gd}$ ) catalysts for the oxidation of carbon monoxide and propane. *J Catal*, 1999, **186**, 147–159.
3. Sanghani, D. V., Abrams, G. R. and Smith, P. J., A structural investigation of some tin-based coloured ceramic pigments. *Trans J Br Ceram Soc*, 1981, **80**, 210–214.
4. Wang, X. and Xie, Y. C., Preparation and characterization of  $\text{SnO}_2$ -based composite metal oxides: active and thermally stable catalysts for  $\text{CH}_4$  oxidation. *Catal Lett*, 2001, **75**(1–2), 73–80.
5. Lopez-Navarrete, E., Caballero, A., Orera, V. M., Lázaro, F. J. and Ocaña, M., Oxidation state and localization of chromium ions in Cr-doped cassiterite and Cr-doped malayaite. *Acta Mater*, 2003, **51**, 2371–2381.
6. Monrós, G., García, A., Sorlí, S., Benet, P. and Tena, M. A., Quantum sized chromophores in vanadium ceramic pigments. *Mater Sci Forums*, 2003, **426–432**, 2423–2428.
7. Tena, M. A., Sorlí, S., Llusar, M., Badenes, J. A., Forés, A. and Monrós, G., Study of Sb-doped  $\text{SnO}_2$  gray ceramic pigment with cassiterite structure. *Z Anorg Allg Chem*, 2005, **631**, 2188–2191.
8. DCMA Classification and Chemical Description of the Mixed Metal Oxide Inorganic Coloured Pigments, 2nd ed. Metal Oxides and Ceramics Colors Subcommittee, Washington DC: Dry Color Manufacturer's Ass.; 1982.
9. Ren, F., Ishida, S., Takeuchi, N. and Fujiyoshi, K., Chromium-based ceramic colors. *Ceram Bull*, 1992, **71**(5), 759–764.
10. Lopez-Navarrete, E., González-Elipé, A. R. and Ocaña, M., Non-conventional synthesis of Cr-doped  $\text{SnO}_2$  pigments. *Ceram Int*, 2003, **29**, 385–392.
11. Cordischi, D., Gazzoli, D., Occhiuzzi, M. and Valigi, M., Redox behavior of VI B transition metal ions in rutile  $\text{TiO}_2$  solid solutions: an XRD and EPR study. *J Solid State Chem*, 2000, **152**, 412–420.
12. Ishida, S., Hayashi, M., Fujimura, Y. and Fujiyoshi, K., Spectroscopic study of the chemical state and coloration of chromium in rutile. *J Am Ceram Soc*, 1990, **73**(11), 3351–3355.
13. Croft, G. and Fuller, M. J., Crystalline oxidic solid-solutions of tin(IV) and titanium(IV), their coloration and thermal reaction with some metals ions. Rutile  $\text{Sn}_x\text{Ti}_{1-x}\text{O}_2$  system and its interaction with V(V), Cr(III), Cr(VI), Mn(II), Fe(III), Co(II), Ni(II), Cu(II) and Sb(III). *Trans J Br Ceram Soc*, 1979, **78**(3), 52–56.
14. Rodriguez-Carvajal, J., *FULLPROF computer program, wfp2ks.exe (January2005-LLB-JRC)*. Laboratoire Leon Brillouin (CEA-CNRS), France, 2001.
15. Commission Internationale de l'Eclairage, "Recommendations on Uniform Color Spaces, Color Difference Equations, Psychometric Color Terms", Supplement no. 2 of CIE Publication No. 15 (E1-1.31); 1971 (Bureau Central de la CIE, Paris, 1978).
16. Monrós, G., Pinto, H., Badenes, J., Llusar, M. and Tena, M. A., Chromium(IV) stabilisation in new ceramic matrices by coprecipitation method: application as ceramic pigments. *Z Anorg Allg Chem*, 2005, **631**, 2131–2135.